IL NUOVO CIMENTO Vol. 35 C, N. 6 Novembre-Dicembre 2012
DOI 10.1393/ncc/i2012-11350-2

Colloquia: LaThuile12

Solar-neutrino physics with Borexino

M. G. Giammarchi(*) on behalf of the Borexino Collaboration
INFN, Sezione di Milano - Milano, Italy

ricevuto il 7 Settembre 2012

Summary. — The Borexino solar-neutrino detector is a high-radiopurity low-threshold liquid scintillator that detects solar neutrinos by means of the elastic scattering $\nu e \to \nu e$ reaction. The detector, located at the Laboratori Nazionali del Gran Sasso (LNGS, Italy) and has now measured solar neutrinos from the ^{7}Be, ^{8}B and pep components. Terrestrial neutrinos (geoneutrinos) have also been observed.

PACS 26.65.+t – Solar neutrinos.
PACS 29.40.Mc – Scintillation detectors.
PACS 14.60.Pq – Neutrino mass and mixing.

1. – Introduction

Solar-neutrino physics originally started from the study of the basic working principle of the core of the Sun, with nuclear-fusion reactions producing energy and emitting neutrinos. The pioneering Davis experiment [1] was the first one to detect (with radiochemical methods) solar neutrinos and to measure a deficit with respect to the flux predicted by theoretical models. Additional experiments were performed starting from the end of the 80's both in radiochemical mode [2-4] and in real-time mode [5-7], while theoretical models of the sun evolved into what is now known as the Standard Solar Model [8,9]. Figure 1 shows the prediction of the flux of solar neutrinos according to the Standard Solar Model.

In general, real-time experiments have been performed with water Cerenkov detectors with an energy threshold of about 5 MeV, mainly due to natural radioactivity. Therefore, only $\sim 0.001\%$ of the total neutrino flux has been observed in real time before 2007.

Measuring low energy (sub-MeV) solar neutrinos has been the subject of an intensive research and development program carried out in Borexino since the beginning of the 90's.

(*) E-mail: marco.giammarchi@mi.infn.it

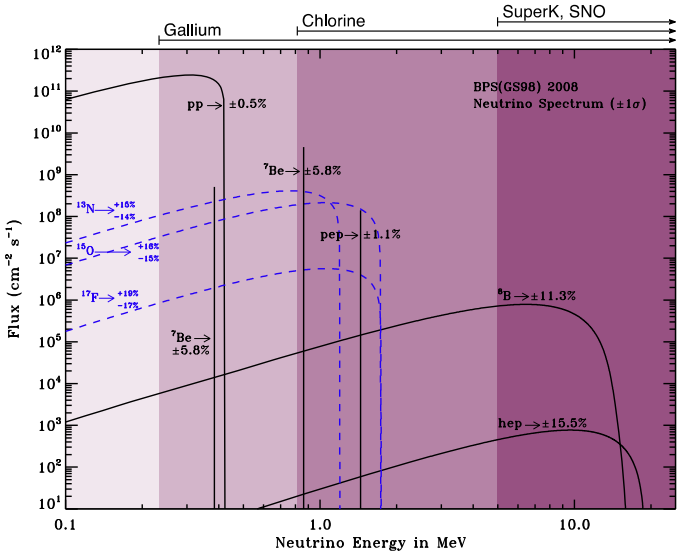

Fig. 1. – Solar-neutrino energy spectrum as predicted by the Sandard Solar Model. Typical detection thresholds of solar-neutrino experiments are shown as well as model uncertainties on the solar fluxes.

Borexino [10] is a real time experiment to study low-energy solar neutrinos and other rare phenomena, based on the $\nu e^- \rightarrow \nu e^-$ elastic scattering reaction. The experimental design threshold is of 50 keV while the analysis threshold is ~ 200 keV; these values make it possible to study solar-neutrino components such as the 0.862 MeV ^{7}Be solar neutrino line, generating a recoil electron with 664 keV maximum energy. The detection reaction is observed in a large mass (100 tons) of ultrapure and well-shielded liquid scintillator.

The predictions of solar fluxes depend both on the Standard Solar Model and the value of the parameters of the LMA solution of neutrino oscillations [11, 12]. The Borexino experimental program makes it possible to directly test this prediction by measuring solar neutrinos on a wide energy range.

The main challenge of an experiment with such a low energy threshold is the background coming from natural sources such as cosmic rays or radioactivity. Studies have been made on low radioactivity materials and purification techniques with a comparable effort devoted to detection and measurement of very low activity levels [13]. As a part of this program, a prototype of the Borexino detector, called Counting Test Facility [14], was built and operated at LNGS to demonstrate very low radioactive contamination levels (10^{-16} g/g of ^{238}U equivalent or less [15]) in a ton scale scintillator detector. This research culminated into the construction, filling and operation of the full-scale Borexino detector.

2. – The Borexino detector

Borexino [16] is an unsegmented scintillation detector featuring ~ 300 tonnes of well-shielded liquid ultrapure scintillator viewed by 2200 photomultipliers (fig. 2). The detector core is a transparent spherical vessel (Nylon Sphere, 100 μm thick), 8.5 m diameter, filled with 300 tonnes of liquid scintillator and surrounded by 100 tonnes of high-purity

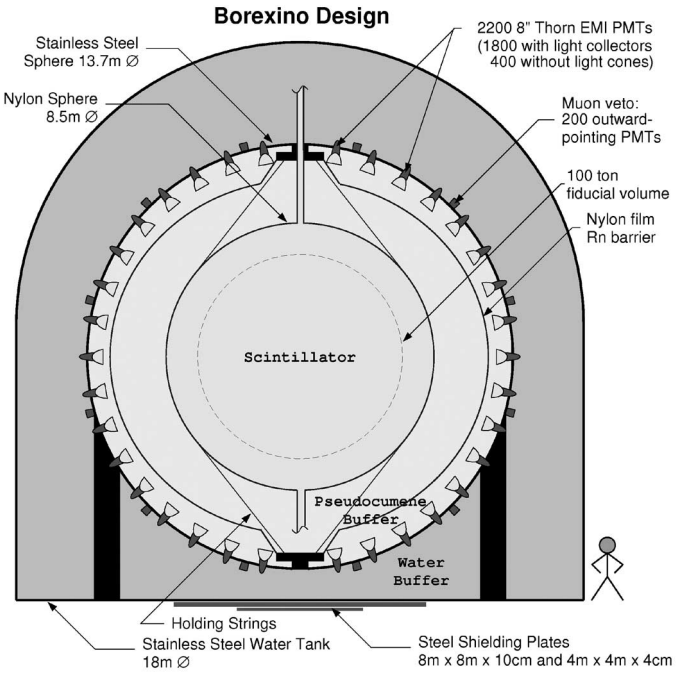

Fig. 2. – Schematics of the Borexino detector at Gran Sasso (see text).

buffer liquid. The scintillator mixture is pseudocumene (PC) and PPO (1.5 g/l) as a fluor, while the buffer liquid consists of PC alone (with the addition of DMP as light quencher). The photomultipliers are supported by a Stainless Steel Sphere, which also separates the inner part of the detector from the external shielding, provided by 2400 tonnes of pure water (Water Buffer). An additional containment vessel (Nylon film Radon barrier) is interposed between the Scintillator Nylon Sphere and the photomultipliers, with the goal of reducing radon diffusion towards the internal part of the detector.

The outer water shield is instrumented with 200 outward-pointing photomultipliers serving as a veto for penetrating muons, the only significant remaining cosmic-ray related background at the Gran Sasso depth (about 3700 m of water equivalent). The innermost 2200 photomultipliers are divided into a set of 1800 devices equipped with light cones (so that they collect light only from the Nylon Sphere region) and a set of 400 PMT's without light cones, sensitive to light originated in the whole Stainless Steel Sphere volume. This design greatly increases the capability of the system to identify muons crossing the PC buffer (and not the scintillator).

The Borexino design is based on the concept of a graded shield of progressively lower intrinsic radioactivity as one approaches the sensitive volume of the detector; this culminates in the use of the 200 tonnes of the low background scintillator to shield the 100 tonnes innermost Fiducial Volume. In these conditions, the ultimate background will be dominated by the intrinsic contamination of the scintillator, while all backgrounds from the construction materials and external shieldings will be neglible.

Borexino also features several external systems conceived to purify the experimental fluids (water, nitrogen, scintillator) used in the experiment (see, *e.g.* [17]).

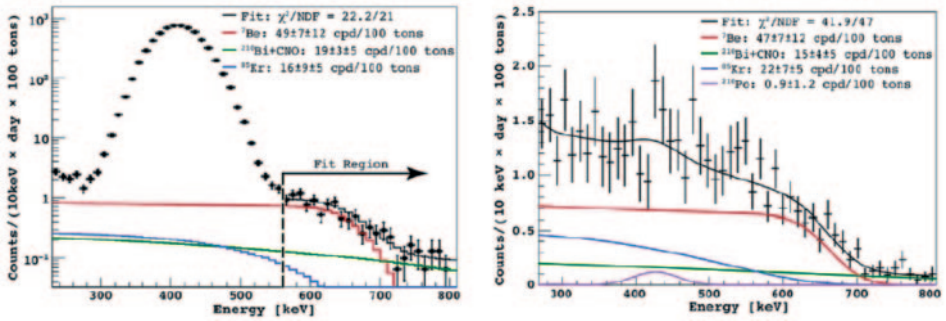

Fig. 3. – The fit to the Be-7 region can be made without (left) or with (right) the statistical α/β discrimination (left). The results of the Be-7 fits in both cases is consistent. The fit is done by including the signal as well as the ^{210}Bi + CNO and the ^{85}Kr background.

3. – Borexino and solar neutrinos

The filling of the detector started in January 2007, with scintillator displacing the purified water from inside the detector volumes. The data taking started in May 2007.

The detection reaction of Borexino, $\nu e^- \to \nu e^-$, is sensitive to all neutrino flavors while having a higher cross section for electron neutrinos. The energy deposited in the active target produces scintillation light which is collected in the photomultipliers. The energy of the event can be reconstructed from the detected number of photoelectrons (~ 500/MeV), while the position of the event is calculated from the photoelectron arrival times. The radiopurity of the detector has been found to be better than the specifications. In particular, ^{14}C contamination of the scintillator was found to be $\sim 2 \times 10^{-18}$ ^{14}C/^{12}C, which is important in the low-energy part of the spectrum (200 keV or less). The Th-232 and U-238 contaminations were found to be $\sim 4.6 \times 10^{-18}$ and $\sim 2 \times 10^{-17}$ g/g respectively. Finally the Kr-85 contamination (of considerable importance for the Be-7 measurement) was limited to 30 counts/day in the Fiducial Volume.

The Borexino main trigger fires when at least 30 PMT's each detect at least a photoelectron within a time window of 60 ns, corresponding approximately to an energy threshold of 60 keV for electrons. The main cuts that are performed in the analysis are the muon cut and the pulse-shape alpha/beta discrimination. Additional cuts involve event quality, delayed coincidences to remove Rn daughters as well as spatial (fiducial) cuts. In all the analyses reported below, only the general characteristics will be given, leaving the interested reader to the full description in the relevant bibliography.

4. – The detection of the Be-7 solar neutrinos

Borexino reported the first detection of solar neutrinos [18] a few months after the start of the data taking. The evidence was based on detecting the recoil spectrum of the electron due to the $\nu e^- \to \nu e^-$ scattering. Figure 3 shows the relevant part of the spectrum after the cuts (quality, muons, space, and Rn daughter cuts, with or without α/β discrimination), with the presence of the ^{210}Po quenched alpha out of equilibrium with the other isotopes of the ^{222}Rn sequence. The ^{210}Po peak is effectively removed by the pulse-shape discrimination cut and the ^{7}Be shoulder (located at 664 keV for a neutrino energy of 861 keV) is evident in the 560–800 keV energy region. This constituted the first experimental evidence of the ^{7}Be nuclear reaction inside the Sun.

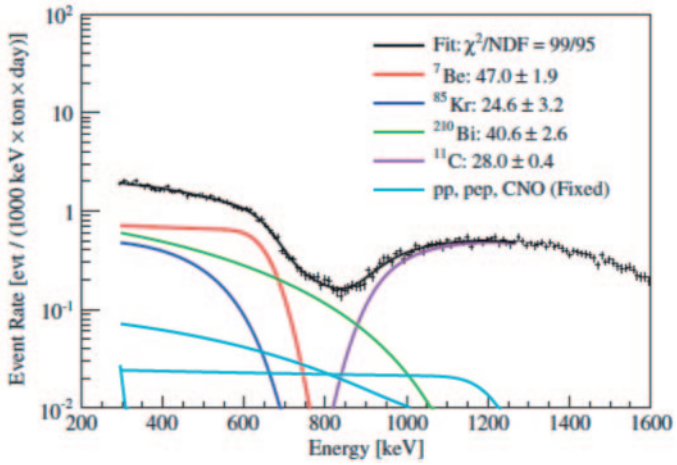

Fig. 4. – Analitically fitted spectrum of recoil electrons in the Be-7 spectral region showing different fit components, given in units of (counts/(day 100 ton)).

During the fit procedures, the backgrounds were left as free parameters, including the ^{85}Kr component, whose spectral shape is similar to the signal and whose uncertainty substantially contributes to the systematic error. We have verified that the ^{85}Kr result from the fit is consistent with the direct measurement of the ^{85}Kr delayed coincidence rate([1]).

Subsequent analyses have profited from better statistics [19] and a subsequent intensive calibration campaign [20] (see below). An example of a fitted spectrum is shown in fig. 4. Again, the Kr-85 fit results was cross-checked with the delayed coincidence measurement. The result obtained for the solar neutrino Be-7 rate is of $46.0 \pm 1.5(\text{stat})^{+1.5}_{-1.6}(\text{syst})$ counts/(day 100 ton), in agreement with the Standard Solar Model and the Mikheyev-Smirnov-Wolfenstein large mixing angle neutrino oscillation mechanism.

As a part of the Borexino solar neutrino data, a study was made to look for day-night asymmetry in the ^{7}Be neutrino rate [21]. The presence of this effect could be indicative of the so-called LOW region of parameters for solar-neutrino oscillations ($\delta m^2 \sim 10^{-7}\,\text{eV}^2$), which was previously strongly disfavored only the KamLAND antineutrino measurement, thereby relying on the CPT assumption. The obtained results, of

$$A_{dn} = 2\,\frac{N-D}{N+D} = 0.01 \pm 0.012(\text{stat}) \pm 0.007(\text{syst}) \tag{1}$$

agrees with the MSW-LMA solution for neutrino oscillations and disagrees with the LOW solution at more than 8.5 σ CL.

([1]) The decay sequence $^{85}\text{Kr} \to {}^{85m}\text{Rb} + \text{e}^+ + \bar{\nu}_\text{e}$, $^{85m}\text{Rb} \to {}^{85}\text{Rb} + \gamma$ ($\tau = 1.5\,\mu$s, BR = 0.43%) was used to tag the content of Kr-85.

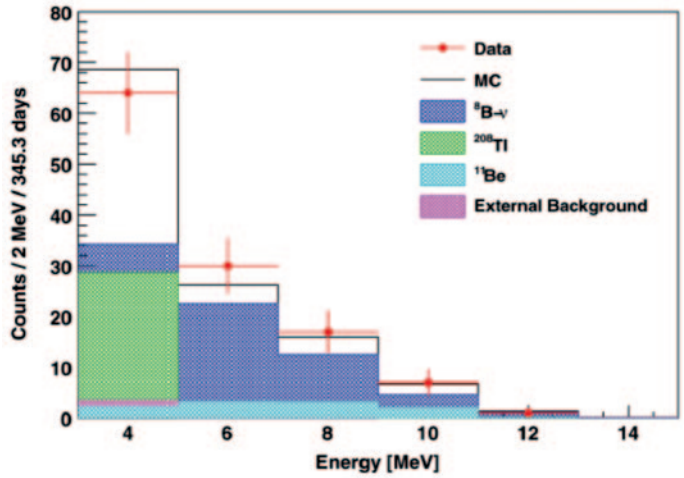

Fig. 5. – ^{8}B neutrino spectrum and remaining background after data selection. The black line is the Monte Carlo simulation.

5. – The calibration campaign

In order to better understand the performance of the detector and minimize systematic error on the ^{7}Be and other measurements, during 2010 an intense calibration campaign was performed. Sources such as ^{57}Co, ^{139}Ce, ^{203}Hg, ^{85}Sr, ^{54}Mn, ^{65}Zn, ^{60}Co, and ^{40}K were used for gamma calibration, while ^{14}C, ^{214}Bi, and ^{214}Po were used to understand the response of the detector to β's and α's. Finally, an AmBe source was used for neutrons and high-energy gammas. These studies allowed a significant reduction of the systematic error on the determination of the Fiducial Volume and the energy scale. Several parameters of the simulation codes (such as the light yield and the quenching factor) could be determined with greater accuracy. External sources were also deployed in several positions around the detector.

In addition, purification campaigns were conducted (water extraction, distillation, nitrogen stripping) that have significantly reduced two of the most important backgrounds, ^{85}Kr and ^{210}Bi.

6. – The B-8 measurement

Solar neutrinos from ^{8}B are measured in Borexino [22] by studying the high-energy part of the spectrum, starting from 3 MeV; this limit is imposed by the presence of the ^{208}Tl contamination. For this analysis, muon and cosmogenic background had to be treated with special care. ^{214}Bi and ^{208}Tl removal were performed together with neutron rejection. Figure 5 shows the final spectrum obtained after the cuts. The fitted number of ^{8}B events, $0.22 \pm 0.04(\text{stat}) \pm 0.01(\text{syst})$ (counts/day 100 t) is in good agreement with the Standard Solar Model (both high and low metallicity) and the MSW-LMA oscilaltion mechanism for neutrinos.

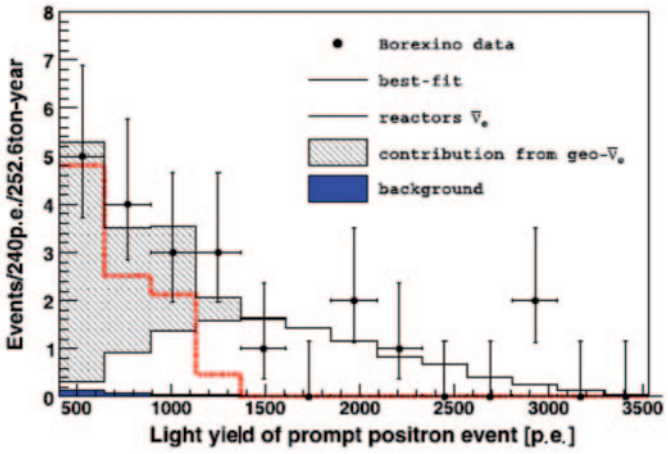

Fig. 6. – Light-yield spectrum for the positron prompt events showing the remaining background, the nuclear reactor component and the geoneutrino signals. The conversion form p.e. to energy is approximately 500 p.e./MeV.

7. – The observation of geoneutrinos

Geoneutrinos, electron antineutrinos produced in β decays of naturally occurring radioactive isotopes in the Earth, are a direct probe of our planet's interior. They are produced in the decays of ^{40}K and in the chains of radioactive isotopes ^{238}U and ^{232}Th. The detection reaction in the Borexino scintillator, $\bar{\nu}_e + p \rightarrow e^+ + n$ (with a 1.806 MeV threshold) makes it possible to detect only a part of the ^{238}U and ^{232}Th antineutrinos. The positron in the final state comes promptly to rest in the scintillator and annihilates by emitting two 511 keV gamma rays, giving a prompt event with a visible energy of $E(\bar{\nu_e}) - 0.782$ MeV, while the free neutron is typically captured on protons with a mean time of 256 μs, resulting in the emission of a 2.22 MeV de-excitation γ-ray which provides a coincident delayed event. Background rejection was performed with special emphasis on accidental coincidences, primary muons producing a secondary neutron and cosmogenically-produced neutron emitters (such as ^{9}Li or ^{8}He).

Thanks to the high radiopurity of the Borexino scintillator, the (α, n) background was small, so the final dominant background after cuts was the one due to European nuclear power reactors, producing antineutrinos up to 10 MeV.

Figure 6 shows the positron spectrum remaining after the cuts, showing the contribution of geo-neutrinos and reactor neutrinos. The geo-neutrino rate was found, though a maximum-likelihhod fit, to be of $3.9^{+1.6}_{-1.3}$ events/100 ton y [23].

8. – The pep first observation and the CNO limit

Observation of solar neutrinos in the 1.0–1.5 MeV energy range poses a special experimental challenge. First of all, ^{11}C background, of cosmogenic origin, is a β^+ emitter that is copiously produced even at the Gran Sasso depth ($\sim$ 30 events/day 100 tons). Secondly, other cosmogenic isotopes like ^{10}C need to be considered. Thirdly, the ^{210}Bi contamination on the low side of the range, needs to be addressed.

This spectral energy range is of great interest for two reasons. First, the pep component of the solar neutrino spectra —a monochromatic 1.44 MeV neutrino line— can be

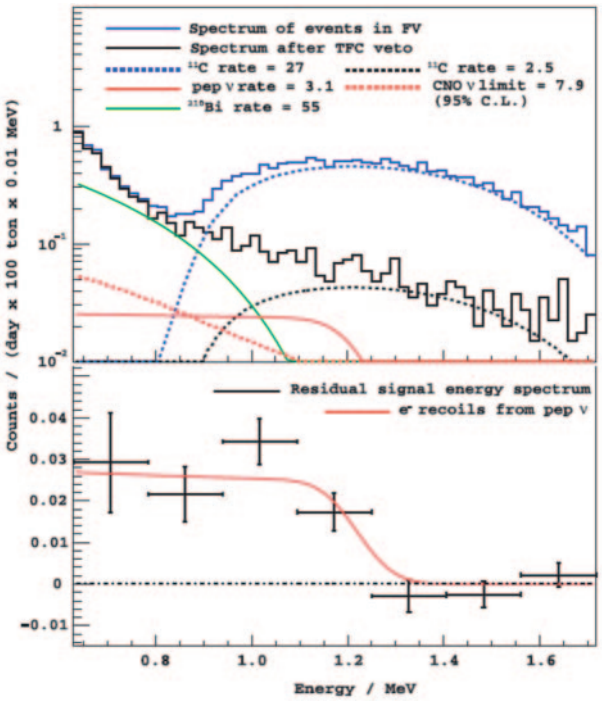

Fig. 7. – Top: energy spectra of events in the Fiducial Volume in the pep region before and after the threefold coincidence. The solid and dashed blue lines show the data and estimated ^{11}C rate before any veto is applied. The solid black line shows the data after the C-11 removal procedure, whose contribution (dashed black line) has been suppressed. The rate values are integrated over all energies and are quoted in units of counts/(day 100 ton). Bottom: residual energy spectrum after best-fit rates of all considered backgrounds are subtracted. The recoil spectrum from pep ν at the best fit rate is also shown.

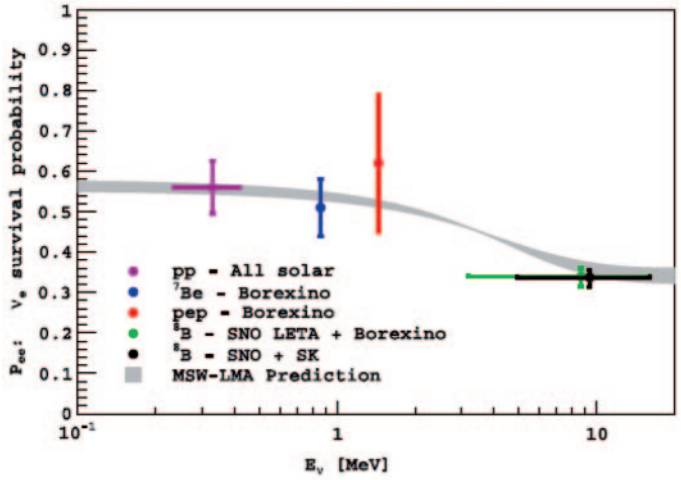

Fig. 8. – Probability that an electron neutrino produced in the Sun will be detected as an eletron neutrino on Earth. The gray band shows the MSW-LMA oscillation prediction.

found in this region; this component is interesting because it occurs at the very beginning of the pp production cycle in the Sun and is therefore well constrained by solar models. Secondly, this range offers the possibility to look for CNO production in the Sun, which is predicted to be $\sim 1\%$ of the pp cycle and has never been observed before.

Similarly to the case of the B-8 analysis, ^{11}C background was reduced by using the threefold coincidence (between the parent muon, a spallation neutron and the ^{11}C beta-plus decay itself). In addition, the pulse-shape difference between e^- and e^+ (from ^{11}C) were measured in organic liquid scintillators; a small difference in the time distribution of the scintillation signals arises in fact from the finite lifetime of the orthopositronium (formed only by the e^+) [25]. This effect was taken into account in the final fit.

Figure 7 shows the spectra before and after the final residual subtraction, with the observation of the pep solar component [24] at $3.1 \pm 0.6(\text{stat}) \pm 0.3(\text{syst})$ counts/(day 100 ton) which agrees with the solar models and the MSW-LMA solution. A pep-CNO correlated analysis was made to study the robustness of the pep result; a CNO flux upper limit was found at < 7.9 counts/(day 100 ton) at 95% CL (pep fixed at the Standard Model value), which is the best upper limit to date.

9. – Conclusions

Borexino has measured the ^{7}Be, pep and ^{8}B solar-neutrino components, therefore decisively contributing to the measurement of the survival probability of solar neutrinos. The survival probability as a function of energy, fig. 8, clearly shows the transition between the vacuum and the matter-dominated energy range. In addition, the detector has measured geoneutrinos at Gran Sasso and imposed upper limits on the day-night asymmetry of the ^{7}Be flux and the CNO component in the Sun.

Finally, the excellent sensitivity of the Borexino detector has been exploited to study additional low-background physics topics [26-28].

Appendix A.

The Borexino Collaboration

G. Bellini, J. Benziger, D. Bick, S. Bonetti, G. Bonfini, M. Buizza Avanzini, B. Caccianiga, L. Cadonati, F. Calaprice, C. Carraro, P. Cavalcante, A. Chavarria, D. D'Angelo, S. Davini, A. Derbin, A. Etenko, K. Fomenko, D. Franco, C. Galbiati, S. Gazzana, C. Ghiano, M. Giammarchi, M. Goeger-Neff, A. Goretti, L. Grandi, E. Guardincerri, S. Hardy, Aldo Ianni, Andrea Ianni, V. Kobychev, D. Korablev, G. Korga, Y. Koshio, D. Kryn, M. Laubenstein, T. Lewke, E. Litvinovich, B. Loer, F. Lombardi, P. Lombardi, L. Ludhova, I. Machulin, S. Manecki, W. Maneschg, G. Manuzio, Q. Meindl, E. Meroni, L. Miramonti, M. Misiaszek, D. Montanari, P. Mosteiro, V. Muratova, L. Oberauer, M. Obolensky, F. Ortica, M. Pallavicini, L. Papp, L. Perasso, S. Perasso, A. Pocar, R. S. Raghavan, G. Ranucci, A. Razeto, A. Re, A. Romani, A. Sabelnikov, R. Saldanha, C. Salvo, S. Schönert, H. Simgen, M. Skorokhvatov, O. Smirnov, A. Sotnikov, S. Sukhotin, Y. Suvorov, R. Tartaglia, G. Testera, D. Vignaud, R. B. Vogelaar, F. von Feilitzsch, J. Winter, M. Wojcik, A. Wright, M. Wurm, J. Xu, O. Zaimidoroga, S. Zavatarelli, and G. Zuzel.

REFERENCES

[1] Davis R., *Nobel Prize Lecture* (2002).
[2] Hampel W. *et al.*, *Phys. Lett. B*, **447** (1999) 127.
[3] Abdurashitov J. N. *et al.*, *Phys. Rev. Lett.*, **83** (1999) 4686.
[4] Altmann M. *et al.*, *Phys. Lett. B*, **616** (2005) 174.
[5] Fukuda S. *et al.*, *Phys. Rev. Lett.*, **86** (2001) 5651.
[6] Fukuda S. *et al.*, *Phys. Rev. Lett.*, **539** (2002) 179.
[7] Ahmad Q. R. *et al.*, *Phys. Rev. Lett.*, **87** (2001) 071301.
[8] Bahcall J. N. and Pinsonneault M. H., *Phys. Rev. Lett.*, **92** (2004) 121301.
[9] Serenelli A. *et al.*, *Astrophys. J. Lett.*, **705** (2009) L123.
[10] Alimonti G. *et al.*, *Astropart. Phys.*, **16** (2002) 205.
[11] Bahcall J. N. *et al.*, *JHEP*, **0408** (2004) 016.
[12] Fogli G. L. *et al.*, *Progr. Nucl. Phys.*, **57** (2006) 742.
[13] Arpesella C. *et al.*, *Astropart. Phys.*, **18** (2002) 1.
[14] Alimonti G. *et al.*, *Nucl. Instrum. Methods A*, **406** (1998) 411.
[15] Alimonti G. *et al.*, *Astropart. Phys.*, **8** (1998) 141.
[16] Alimonti G. *et al.*, *Nucl. Instrum. Methods A*, **600** (2009) 568.
[17] Alimonti G. *et al.*, *Nucl. Instrum. Methods A*, **609** (2009) 58.
[18] Arpesella C. *et al.*, *Phys. Lett. B*, **658** (2008) 101.
[19] Arpesella C. *et al.*, *Phys. Rev. Lett.*, **101** (2008) 091302.
[20] Bellini G. *et al.*, *Phys. Rev. Lett.*, **107** (2011) 141302.
[21] Bellini G. *et al.*, *Phys. Lett. B*, **707** (2012) 22.
[22] Bellini G. *et al.*, *Phys. Rev. D*, **82** (2010) 033006.
[23] Bellini G. *et al.*, *Phys. Lett. B*, **687** (2010) 299.
[24] Bellini G. *et al.*, *Phys. Rev. Lett.*, **108** (2012) 051302.
[25] Franco D. *et al.*, *Phys. Rev. C*, **83** (2011) 015504.
[26] Bellini G. *et al.*, *Phys. Lett. B*, **696** (2011) 191.
[27] Bellini G. *et al.*, *JINST*, **6** (2011) P05005.
[28] Bellini G. *et al.*, *Phys. Rev. D*, **85** (2012) 092003.